I

Publication I

Backman J, Oksanen T, Visala A.

Navigation System for Agricultural Machines: Nonlinear Model Predictive Path Tracking.

Computers and Electronics in Agriculture. 82, 32-43

Computers and Electronics in Agriculture 82 (2012) 32–43

Contents lists available at SciVerse ScienceDirect

Computers and Electronics in Agriculture

journal homepage: www.elsevier.com/locate/compag

Navigation system for agricultural machines: Nonlinear Model Predictive path tracking

J. Backman *, T. Oksanen, A. Visala

Aalto University, School of Electrical Engineering, Department of Automation and Systems Technology, P.O. Box 15500, 00076 Aalto, Finland

ARTICLE INFO

Article history:
Received 16 February 2011
Received in revised form 30 November 2011
Accepted 20 December 2011

Keywords:
Navigation
Implement guidance
Path tracking
Nonlinear Model Predictive Control
Kinematics

ABSTRACT

This article presents a new kind of navigation system for agricultural machines. The focus is on trajectory control where a Nonlinear Model Predictive path tracking for tractor and trailer system is presented. The experiments of the proposed method are carried out by using real agricultural machines in real environments.

The agricultural objective is to drive so that swaths are exactly side-by-side, without overlapping or gaps. Hence, the objective of this research was to control the lateral position of the towed implement and to keep it close to the adjacent driving line. The adjacent driving line was recognized locally by using a 2D laser scanner. The local measurement and global position information was merged with the help of an Extended Kalman Filter (EKF). The measurement of the heading by GPS was improved by using an inertial measurement unit and a separate EKF filter. The position of the implement was controlled by steering the tractor and by the use of a hydraulically controlled joint. Because there were two actuators which affected the position of the implement, the problem was a multivariable control problem. Nonlinear Model Predictive Control (NMPC) was used to accomplish the navigation task.

The goal was to build a system, which is able to have at least the same accuracy as a human driver. The sufficient accuracy requirement was at most 10 cm lateral error at a speed of 12 km/h. The results presented in the article show that the goal was met and NMPC is a feasible method for accurate path tracking. Further investigation is, however, needed to adapt the method to other kinds of agricultural machines.

1. Introduction

In a recent survey, different existing path tracking methods were extensively compared (Snider, 2009). The path tracking methods were classified into three groups: the geometric approach, the kinematic control laws and the optimal control. Model Predictive Control (MPC) and its extension, Nonlinear Model Predictive Control (NMPC), were seen as the next logical evolutionary step in that survey.

The goal of the autonomous navigation or guidance in agriculture is to control the trajectory of the vehicle, to keep it within a constant distance to the adjacent driving line, or as in agricultural terms, to lay swaths side by side. Although the tractor and implement could be located differently, most commercial guidance systems concentrate on keeping the tractor at a constant distance from the adjacent driving line. Actually, the objective should rather be to keep the operational point in the implement, like coulters in a seed drill or nozzles in the sprayer, at the constant distance from the adjacent driving line. Especially in curves, a trailer does not follow the same track as the tractor does and the tractor alone for navigation will result in gaps and overlaps.

In order to be useful, the autonomous navigation system must be able to drive as fast as human driver and be at least as accurate as a human. Most of the autonomous systems drive at much slower speeds than traditional agricultural working machines or achieve less accuracy when operated at higher speeds. In this research the goal was to build a tractor–trailer navigation system which is able to drive at a speed of at least 12 km/h with less than 10 cm lateral error. This speed is sufficient for most agricultural operations that require high precision. A real-time solution was also required in order to experimentally evaluate the system under real field conditions.

The remaining part of this article is organized in following way. Firstly is presented, a brief review of studies on path tracking using MPC and NMPC methods, and studies about path tracking with tractor–trailer systems. Secondly, the configurations for tests, the derivation of the kinematic model of the tractor–trailer system and the dynamic model of the actuators used in this study are explained. After that, the NMPC method and the required state

* Corresponding author. Tel.: +358 9 470 25154; fax: +358 9 470 23308.
E-mail address: juha.backman@aalto.fi (J. Backman).

0168-1699/$ - see front matter © 2012 Elsevier B.V. All rights reserved.
doi:10.1016/j.compag.2011.12.009

estimations are described. Finally, the experimental results of the navigation system are reported and some conclusions are highlighted.

1.1. Studies of Model Predictive Controller and path tracking

Nonlinear Model Predictive Controllers are normally used in industrial plants and in process control to optimize the operation points of the controlled process. It is easier to implement NMPC in these environments due to longer time constants. If the time constants of the system are smaller as in vehicle trajectory control, the controller must run with a higher control cycle. This demands high computing capacity for real time control. However, in the last 10 years or so, the development in computational capacity of desktop processors and also the development in numerical methods to solve the optimization problems have made it possible to use the NMPC in real-time solutions for mobile robots. Research conducted on the usage of the MPC for the path or trajectory tracking purposes is sparse and those available mostly deal with the computational requirements.

One way to lighten the computational requirements is to combine MPC and another control law that actually do the steering of the vehicle. The purpose of MPC is to improve the performance of the complementing control law. Kim et al. (2001) used MPC for avoiding wheel-ground slippage and loss of wheel-ground contact. The method was proven to work in experiments with a three-wheeled vehicle on an inclined surface. Another research where MPC was used to improve the performance of another control technique was carried out by Lenain et al. (2005). In the research, MPC was used in the real-time control of the steering angle of the tractor. The desired steering angle was calculated by a nonlinear control law from the followed path. The MPC was used to reduce the "delay phenomenon" of the actual steering system.

In the development of automotive safety systems, Keviczky et al. (2006) used NMPC to stabilize the vehicle along a desired path while reducing the effect of wind gusts. The commercial NPSOL software package was used in the tests. The vehicle speed was varied from 5 to 17 m/s. It was found that when the driving speed was increased, the corresponding control and prediction horizons must be increased dramatically in order to achieve stable performance. This increase then leads to problems in computational complexity. To reduce the computational complexity, a suboptimal MPC controller based on successive online linearization of the nonlinear vehicle model (LTV MPC) was later presented in Falcone et al. (2007). The resulting optimization problem was recast to a quadratic program (QP) and solved with Model Predictive Control Toolbox for Matlab available from The MathWorks Incorporated. It was found that the LTV MPC was able to stabilize the vehicle, even at high speeds, although the control horizon was reduced to one.

Kühne et al. (2005a) presented nonlinear MPC and linear MPC methods used to solve path tracking problem on a nonholonomic wheeled mobile robot. In their research, the computational effort required to solve the optimization problems was studied and the performance of both controllers were compared. They found out that at the time of their research that, the Nonlinear Model Predictive Controller was computationally too demanding to be solved in real-time with a prediction horizon larger than 5 and also that the linear MPC had a good performance with lower computational effort. But they also noted that the linear model is only valid near the reference trajectory. Furthermore, Kühne et al. (2005b) proposed an alternative way to formulate a cost function. The modified cost function was calculated in polar coordinates and the weight of the state cost increased among the prediction horizon. With this modified cost function, the computational effort was reduced and a better steady state performance was achieved.

Vougioukas (2007) used nonlinear MPC (NMPC) to control the steering angle and the speed of their vehicle. The criterion was the difference between the desired path and the predicted path. Although experiments were done completely in a simulator, good results were achieved and the advantage of this approach was shown.

Klančar and Škrjanc (2007) proposed a tracking-error model-based predictive control law for tackling the trajectory tracking problem for a nonholonomic wheeled mobile robot. The prerequisite was that the reference path should be a smooth twice-differentiable function of time. The control law was based on a linearized error dynamics model obtained around the reference trajectory. The resulting control law was analytically derived and therefore computationally light.

It is well know that the MPC is not guaranteed to be stable due to the finite prediction horizon. Gu and Hu (2006) developed a method to calculate the terminal state region and a corresponding controller for ensuring the stability of the controller. However, the proposed controller needed a feasible initial solution. Also the computational efficiency was noted to be a problem and worthy of further investigation.

1.2. Studies of path tracking with tractor–trailer system

All the approaches mentioned before are purposed for robot-only navigation. In the literature there are, however, numerous proposals for control laws for tractor–trailer systems. Most of the studies concern reverse motion with a trailer, because forward motion is seen to be naturally exponentially stable. According to Cariou et al. (2010) and Siew et al. (2009) these control laws are not well-adopted for an agricultural context due to delays and nonlinearities in actuators and sliding conditions of varying soils. Cariou et al. (2010) studied headland manoeuvres with a trailer. Model Predictive Control was used to anticipate speed variations and reject significant overshoots in longitudinal motion in the same manner as in Lenain et al. (2005). However, the trailer was again ignored in forward motion and, in backward motion, the objective is to maintain a constant joint angle between the tractor and trailer.

Siew et al. (2009) modelled the behaviour of a tractor-implement-trailer (tractor with two trailers and the first trailer was controlled by steering its wheels) system with sliding conditions. The controller for the trailer was not constructed. However, the impractical assumption of slippage free motion was shown in this study. Also, Karkee and Steward (2010) studied the characteristics of a tractor and a single axle towed implement system. In the paper, three different models for a tractor–trailer system were derived: kinematic model, dynamic model and high-fidelity model. In the last model, the tire relaxation length was included into the dynamic model. The experiments showed that the kinematic model described the behaviour sufficiently well when the driving speed was less than 4.5 m/s and input frequency less than 1 rad/s. A high-fidelity model was needed when the driving speed was increased. In the paper, the closed loop behaviour with the Linear Quadratic Regulator (LQR) was also studied. The controller was used to stabilize the tractor and implement heading errors as well as the tractor lateral error. The controller was unstable at 4.5 m/s forward velocity when the kinematic model was used. With the high-fidelity model the controller was stable for a range of 0.5–10.0 m/s forward velocities. However, it was noticed that the linearization of the model does not hold when the steering or heading angle was above 10 deg. The LQR control has been used also in other tractor–trailer experiments (e.g. Bevly, 2001; Bell, 1999).

There are even commercial solutions for tractor–trailer navigation, for example John Deere's iGuide and iSteer (Deere, 2009a,b). The difference between these systems is that iGuide is based on passive implement control (the implement does not have any

steering mechanism) and iSteer is based on active implement control (the implement has its own steering system). However, it seems that both of these systems are add-ons for basic tractor-only guidance system. In iGuide, the roll angle of the machine is monitored and slipping due to the slope is compensated by setting an offset from the path in the tractor navigation. The offset value is directly proportional to the roll angle. In iSteer, both, the tractor and the trailer, are kept on the desired path. The trailer has its own positioning and steering systems. In this manner, the tractor–trailer system has two separate navigation systems that have a common user interface. It seems that both of these systems are intended to be used mainly on straight driving lines.

Other manufactures have similar products also. An example is the Trimble TrueGuide system. However, it seems that all these products use either two separate controllers (tractor and implement have their own) or an implement error is used directly as an offset value for tractor-guidance. A drawback of these solutions is that the trailer navigation does not take into account the deviations from the desired path caused by the tractor navigation and vice versa. This control problem is truly a multivariate nonlinear control problem and more advanced control systems can be used to improve the accuracy of the navigation system.

2. The test configuration

In this article, the test configuration consisted of a standard tractor and a towed trailer type implement. The tractor and the trailer were equipped for the navigation tests with position measurement and control devices. A mathematical model, described in Section 2.2, is needed both for estimation and control of the tractor–trailer system. The NMPC uses the mathematical model to predict or estimate the future in the optimization process. The Extended Kalman Filter (EKF) uses the same model to estimate the current state of the controlled system.

2.1. Equipments

The test configuration was the same as reported in (Backman et al., 2009). The tractor was a *Valtra T190*, with added *ISO 11783 Class 3* functionalities. The trailer was a *Junkkari Maestro 3000* seed drill equipped with an *ISO 11783* implement controller. The drawbar of the seed drill was modified by adding an extra controllable angle joint, which gave an extra degree of freedom for guidance of the vehicle. The test configuration for the tractor and towed trailer, i.e. the vehicle, is presented in Fig. 1.

The tractor and towed trailer had two sensor systems for measuring the distance to the adjacent driving line: a *global* GPS-based on the tractor and a *local* laser scanner-based located on the implement-side. In this research, a Timble 5700 VRS-GPS together with a Xsens Technologies MT9-B inertial measurement unit (IMU) were used for global localisation and a Sick LMS221 2D laser scanner was used for local localisation. The Sick LMS221 pointing downwards, scans a 180 deg area with 1 deg resolution 77 times per second. The seed drill had a small *marking plough* mounted on the trailing harrow at the rear right corner of the seed drill. The marking plough produced a small furrow, which was identified from the field profile measurement by the laser scanner. The local measurement and the global position information were merged with the help of the Extended Kalman Filter and a kinematic model.

The tractor with *ISO 11783 Class 3* functionality made it possible to control the speed and the steering angle of the tractor through the Controller Area Network bus (CAN-bus). The guidance computer was assembled from standard components of a desktop computer. The components; an Intel DG45FC Mini-ITX Motherboard, Intel Core 2 Duo E8600 processor and 2GB memory were installed in a self-made rugged pc case. The navigation computer was connected to an *ISO 11783* CAN-bus through which commands and most measurements were transferred. The transfer rate of the messages was limited to 100 ms due to the requirements of the *ISO 11783* standard, and the capabilities of the VRS-GPS and the hydraulic valves.

2.2. Model of the tractor–trailer system

The tractor–trailer system could be modelled with a dynamic model, in which every force that affects the system is considered. Such a model would describe the reality perfectly. However, tuning this kind of model would be difficult and taking care of all the circumstances and the forces is impossible as it would also require modelling of the environment. For example slipping depends on soil moisture and tyre properties, slope at the current position, whether the implement is engaged with the soil or not, and amount of additional weights installed on. Furthermore, by using this kind of model with the NMPC would lead to difficulties with computational capacity. For these reasons, some simplifying assumptions were made in the development of the model.

In derivation of the kinematic model, it is assumed that the ground is ideal and slipping affects only the front steering wheels sideways. By these assumptions the kinematic model of the tractor is similar to the well-known bicycle model. The difference is an added slipping factor. The kinematic model of the tractor is given in Eq. (1).

$$\begin{bmatrix} \dot{x}_R \\ \dot{y}_R \\ \dot{\theta} \\ \dot{\delta} \end{bmatrix} = \begin{bmatrix} v_t \cos\theta \\ v_t \sin\theta \\ v_t \frac{\tan\delta\alpha_t}{a} \\ 0 \end{bmatrix}, \tag{1}$$

where (x_R, y_R) is the centre position of the rear axle, θ is the heading angle, δ is the slipping factor, α_t is the realized steering angle, v_t is the realized vehicle speed and a is the wheelbase.

Fig. 1. The test configuration consisted of a standard tractor and towed trailer.

In literature (e.g. Wong, 2008, pp. 30–39), the tyre slipping is usually modelled by introducing a slip angle which is added to the steer angle; $\alpha = \alpha_t + \alpha_{slip}$, where α is the effective steering angle. Then the slip angle α_{slip} will constantly change especially in curves. If there are no external forces pulling or pushing the tractor sideways, it can be assumed that the slipping is caused by inertia and the slipping angle is approximately relative to the steering angle. By introducing the slipping factor, the slip angle can be relatively calculated from the steer angle; $\alpha_{slip} = (\delta - 1)\alpha_t$, if the steering angle is not equal to zero. If the conditions remain the same, the slipping factor is somewhat constant despite the changes in the steering angle.

Because both, the EKF and the NMPC, work in discrete time, Eq. (1) is discretized with Euler's approximation:

$$\begin{bmatrix} x_R(t_{k+1}) \\ y_R(t_{k+1}) \\ \theta(t_{k+1}) \\ \delta(t_{k+1}) \end{bmatrix} = \begin{bmatrix} x_R(t_k) + v_t(t_k)\cos\theta(t_k)T \\ y_R(t_k) + v_t(t_k)\sin\theta(t_k)T \\ \theta(t_k) + v_t(t_k)\frac{\tan\delta(t_k)\alpha_t(t_k)}{a}T \\ \delta(t_k) \end{bmatrix}, \tag{2}$$

where the sampling period is constant; $t_{k+1} - t_k = T$. In this research $T = 100$ ms sampling period was used due to limits of the communication network.

The behaviours of the tractor actuators were modelled as first order dynamic models. It is assumed that the actuators were able to realize the desired control values eventually and no steady state errors were present. The realized control values or the states where the actuators are currently located are modelled according to Eq. (3) as:

$$\begin{bmatrix} v_t(t_{k+1}) \\ \alpha_t(t_{k+1}) \end{bmatrix} = \begin{bmatrix} k_v v_t(t_k) + (1 - k_v) v_d(t_k) \\ k_\alpha \alpha_t(t_k) + (1 - k_\alpha)\alpha_d(t_k) \end{bmatrix}, \tag{3}$$

where k_v and k_α are the dynamic coefficient parameters v_d and α_d and are the desired control values, which are fed to the actuators, the desired speed and steering angle, respectively.

If it is assumed that the trailer does not slide sideways, the kinematic behaviour of the trailer can be modelled with only the angle between the trailer and the tractor. The differential equation of the freely moving joint angle is given in Eq. (4) (derived in Backman et al., 2009).

$$\dot{\beta} = \frac{-a v_t \sin(\beta + \gamma_t) + v_t(d + c\cos\gamma_t + b\cos(\beta + \gamma_t))\tan\alpha_t - ad\dot{\gamma}_t}{a(d + c\cos\gamma_t)}, \tag{4}$$

where β is the angle between the tractor and the trailer, γ_t is the realized angle of the controlled joint, d is the distance to the seed coulters from the drawbar, c is the length of the drawbar and b is the distance to the attachment point from the rear axle. The differential equation is again discretized with Euler's approximation:

$$\beta(t_{k+1}) = \beta(t_k) + \dot{\beta}(t_k)T. \tag{5}$$

The realized control value is modelled with first order dynamic model:

$$\gamma_t(t_{k+1}) = k_\gamma \gamma_t(t_k) + (1 - k_\gamma)\gamma_d(t_k), \tag{6}$$

where k_γ is the filter coefficient and γ_d is the desired joint angle.

There are also auxiliary states for the optimization and the estimation process. The centre position of the trailer is needed for the cost function in the NMPC. The trailer position is modelled with Eq. (7):

$$\begin{bmatrix} x_E \\ y_E \end{bmatrix} = \begin{bmatrix} x_R - b\cos\theta - c\cos(\beta - \theta) - d\cos(\beta + \gamma_{actual} - \theta) \\ y_R - b\sin\theta + c\sin(\beta - \theta) + d\sin(\beta + \gamma_{actual} - \theta) \end{bmatrix}, \tag{7}$$

where (x_E, y_E) is the centre position of the trailer and d is the distance from the drawbar.

The location of the laser scanner and the marking plough are needed for the local correction of the position of the vehicle with the laser scanner measurement. The position of the laser scanner is calculated as:

$$\begin{bmatrix} x_L \\ y_L \end{bmatrix} = \begin{bmatrix} x_E + l_x\cos(\beta + \gamma_{actual} - \theta) - l_y\sin(\beta + \gamma_{actual} - \theta) \\ y_E - l_x\sin(\beta + \gamma_{actual} - \theta) - l_y\cos(\beta + \gamma_{actual} - \theta) \end{bmatrix}, \tag{8}$$

where (x_L, y_L) is the position of the laser scanner l_x and is the axial and l_y the cross-axial distance from the centre position of the trailer. The position of the marking plough is calculated in Eq. (9) as:

$$\begin{bmatrix} x_P \\ y_P \end{bmatrix} = \begin{bmatrix} x_E + p_x\cos(\beta + \gamma_{actual} - \theta) - p_y\sin(\beta + \gamma_{actual} - \theta) \\ y_E - p_x\sin(\beta + \gamma_{actual} - \theta) - p_y\cos(\beta + \gamma_{actual} - \theta) \end{bmatrix}, \tag{9}$$

where (x_P, y_P) is the position of the marking plough and p_x is the axial and p_y the cross-axial distance from the centre position of the trailer.

The resulting state vector of the overall kinematic model is:

$$x = [\, x_r \quad y_R \quad \theta \quad \delta \quad v_t \quad \alpha_t \quad \beta \quad \gamma_t \quad \dot{\gamma}_t \quad x_E \quad y_E \,]^{\mathrm{T}}, \tag{10}$$

and the overall resulting control vector is:

$$u = [\, v_d \quad \alpha_d \quad \mu_d \,]^{\mathrm{T}}. \tag{11}$$

Subsequently, the system model is given as:

$$x(t_{k+1}) = f(x(t_k), u(t_k)), \tag{12}$$

where function f includes Eqs. (2), (3) and (5)–(7).

Because the derivative of the joint angle is needed in Eq. (3), the optimized control value is actually $\dot{u}$ and u is obtained by integration. This gives also an ability to limit the derivatives of the control values without numerical derivations.

The states and parameters of the system are visualized in Fig. 2.

3. Nonlinear Model Predictive Control

The basic idea of the NMPC is to predict the future states of the system and to minimize the given cost function. The future is predicted with the mathematical model of the controlled system (Eq. (12)) by applying the control values to the system model in an open loop manner. The cost function is a weighted quadratic sum of the state and the control values. The general form of the cost function at time t_k is:

$$J(t_k) = \sum_{j=1}^{M} \|x(t_{k+j}|t_k) - r_x(t_{k+j})\|_Q^2 + \sum_{j=1}^{M} \|u(t_{k+j}|t_k) - r_u(t_{k+j})\|_{R_1}^2 + \sum_{j=1}^{M} \|\dot{u}(t_{k+j}|t_k)\|_{R_2}^2, \tag{13}$$

where M is the prediction horizon size, $x(t_{k+j}|t_k)$ is the predicted state for the future time t_{k+j} at the time t_k, r_x is the reference trajectory for state and r_u is the reference trajectory for the controls. In the function, Q, R_1 and R_2 are symmetric positive semi-definite weighting matrices. The optimization problem can then be formulated to find the sequence of controls such that:

$$\dot{u}^*(t_k \cdots t_{k+M}|t_k) = \underset{\dot{u}}{\operatorname{argmin}} J(t_k), \tag{14}$$

where $\dot{u}^*(t_k \cdots t_{k+M}|t_k)$ is the sequence of the optimal control values at time t_k. Only the first control values are used for the actual control and the optimization is repeated with the new state estimates at the time t_{k+1}. The constraints of the optimization problem are obtained from the system model, and the constraints of the states and control values as:

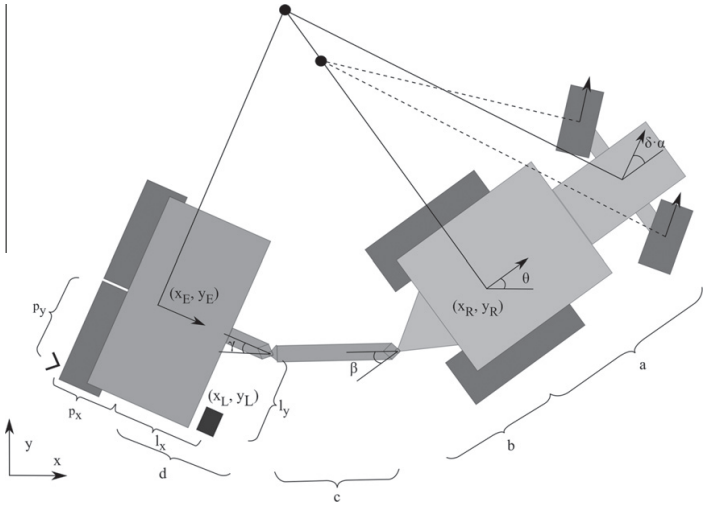

Fig. 2. Variables and parameters of the kinematic model.

$$
\begin{aligned}
&x(t_{k+j+1}|t_k) = f(x(t_{k+j}|t_k), u(t_{k+j}|t_k))\\
&u(t_{k+j+1}|t_k) = u(t_{k+j}|t_k) + \dot{u}(t_{k+j}|t_k)T\\
&x_{min} \leqslant x(t) \leqslant x_{max},\ \forall t \in (t_k, t_{k+M})\\
&u_{min} \leqslant u(t) \leqslant u_{max},\ \forall t \in (t_k, t_{k+M})\\
&\dot{u}_{min} \leqslant \dot{u}(t) \leqslant \dot{u}_{max},\ \forall t \in (t_k, t_{k+M}),
\end{aligned}
\tag{15}
$$

where x_{min} and x_{max} are the minimum and the maximum values of the states, u_{min} and u_{max} are the minimum and the maximum values of the control values and $\dot{u}_{min}$ and $\dot{u}_{max}$ are the maximal decreases and the maximal increases of the control values.

3.1. From trajectory tracking to path tracking

The natural and easy way to use NMPC is to implement a trajectory tracking controller. In trajectory tracking, desired trajectory is explicitly used in the cost function of NMPC (Eq. (13)). In this research, however, the goal was to investigate path tracking methods. The first part of the cost function (state penalty) is visualized in Fig. 3. The difference between the control points and the desired path is penalized. Therefore, the trajectories r_x and r_u are not constant and fixed to the time. The $r_x(t_{k+j})$ is calculated at each Sequential Quadratic Programming (SQP) iteration such that it minimizes the distance of $x(t_{k+j}|t_k)$ from the path. The $r_u(t_{k+j})$ is calculated such that it corresponds to the position of the $r_x(t_{k+j})$ in the path. The state trajectory is calculated both for the tractor and for the trailer separately. In the following equations, the trajectory is calculated for the tractor. The same equations hold for the trailer, but the state components $(x_{\{x_R,y_R\}})$ are changed to correspond to the trailer's state $(x_{\{x_E,y_E\}})$.

The target path is modelled as a polyline. The distance between consecutive points in the path is considered to be constant. Also, the orientation of the tractor along the path and desired velocity and steering angles (i.e. steady state controls) are incorporated into the path points. First, the path point (P_i) that is closest to the current state $x_{\{x_R,y_R\}}(t_{k+j}|t_k)$ is searched:

$$
i = \operatorname{argmin}_i \|x_{\{x_R,y_R\}}(t_{k+j}|t_k) - P_i\|^2. \tag{16}
$$

In the searching procedure, it is assumed that the local minimum, which is found near to the minimum of the previous time step, is also the global minimum.

Then the distances of the state from the line $P_{i-1} - P_i$ and from the line $P_i - P_{i+1}$ are calculated. In addition, the corresponding closest points and the derivatives of the distances with respect to the state are also calculated.

To clarify the equations, the following shorthand notations are used: point X corresponds to the state $x_{\{x_R,y_R\}}(t_{k+j}|t_k)$, A corresponds to P_i and B corresponds to P_{i+1}. XA is the line segment from X to A, BX is the line segment from B to X and AB is the line segment from A to B. Finally, the subscript $\cdot_x$ or $\cdot_y$ represents the x or y component of the corresponding line segment or point. With these shorthand notations the distance (d_*) of the X from the AB is:

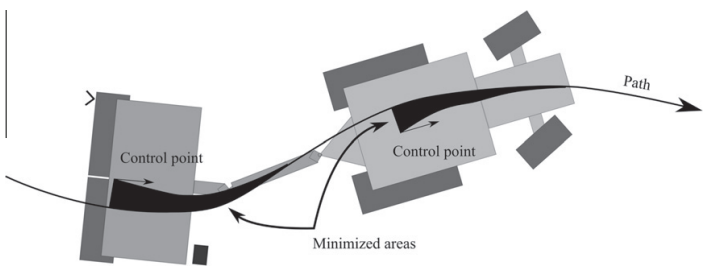

Fig. 3. The visualization of the state penalty in the NMPC cost function.

$$d_+ = \frac{X_x \cdot (AB)_y - B_x \cdot (AX)_y + A_x \cdot (BX)_y}{\sqrt[2]{\|AB\|^2}}. \quad (17)$$

Equally, the position of the closest point (r_x) along the line segment AB is:

$$t_+ = \frac{(AX)_x \cdot (AB)_x + (AX)_y \cdot (AB)_y}{\|AB\|^2}, \quad (18)$$

where the value $t_+ = 0$ means that $r_x = A$ and the value $t_+ = 1$ means that $r_x = B$.

The derivatives of the distance d_+ with respect to the state are:

$$\frac{\delta d_+}{\delta X_x} = \frac{(AB)_y}{\sqrt[2]{\|AB\|^2}}, \quad (19)$$

and

$$\frac{\delta d_+}{\delta X_y} = \frac{-(AB)_x}{\sqrt[2]{\|AB\|^2}}. \quad (20)$$

To calculate the distances (d_- and t_-) from the line $P_{i-1} - P_i$, the shorthand notations are changed such that B corresponds to P_{i-1}. Because the order of path points changes, the sign of the distance d_- and the corresponding derivatives also changes and must be compensated in equations.

If the distances between the path points are close to constant, there are four different cases to be used calculate the closest position from the path: Case 1: position X is closest to the line segment $P_{i-1} - P_i$, Case 2: position X is closest to the line segment $P_i - P_{i+1}$, Case 3: position X is closest to path point P_i and Case 4: the inner curve (Fig. 4). In Case 1 ($t_- \in (0,1) \wedge t_+ < 0$), d_- and corresponding derivatives can be directly used in the cost function. Equally, in Case 2 ($t_+ \in (0,1) \wedge t_- < 0$), d_+ and corresponding derivatives can be directly used in the cost function. In Case 3 ($t_- < 0 \wedge t_+ < 0$), P_i is used as a trajectory point r_x. In Case 4 ($t_+ \in (0,1) \wedge t_- \in (0,1)$), the weighted average of d_+ and d_- is used, by using the t_+ and t_- as weighting factors. The weighting makes the path smoother, though the weighted distance to the path is not equal to the actual shortest distance.

In Cases 1, 2 and 4, there is no need to explicitly calculate the trajectory point r_x, since the part of the cost function is:

$$\|x_{\{x_R,y_R\}}(t_{k+j}|t_k) - r_{x_{\{x_R,y_R\}}}(t_{k+j})\|_Q^2 = d^2 Q_{\{x_R,y_R\}}, \quad (21)$$

where $Q_{\{x_R,y_R\}}$ is the weighting factor of the corresponding states. And the partial derivatives of the cost with respect to the state elements are:

$$\frac{\delta J(t_k)}{\delta x_{\{x_R\}}(t_{k+j}|t_k)} = 2dQ_{\{x_R\}} \frac{\delta d}{\delta x_{\{x_R\}}(t_{k+j}|t_k)}, \quad (22)$$

and

$$\frac{\delta J(t_k)}{\delta x_{\{y_R\}}(t_{k+j}|t_k)} = 2dQ_{\{y_R\}} \frac{\delta d}{\delta x_{\{y_R\}}(t_{k+j}|t_k)}. \quad (23)$$

The partial derivatives used in Eqs. (22) and (23), are calculated in Eqs. (19) and (20) with the shorthand notations.

3.2. Numerical solution of the optimization problem

There are many different methods for solving the previously described constrained nonlinear optimization problem. One commonly used numerical method is Sequential Quadratic Programming (SQP) (Schittkowski, 1983). There are many implementations of the method in different packages. In this research, a Nonlinear Model Predictive Control Tool called HQP (Huge Quadratic Programming) was selected (Franke and Arnold, 1997, 2008). HQP has been used successfully, for instance, in batch process control (Nagy et al., 2007), energy systems and water systems. It solves nonlinearly constrained problems with SQP algorithm. Convex quadratic sub problems (QP) are solved with

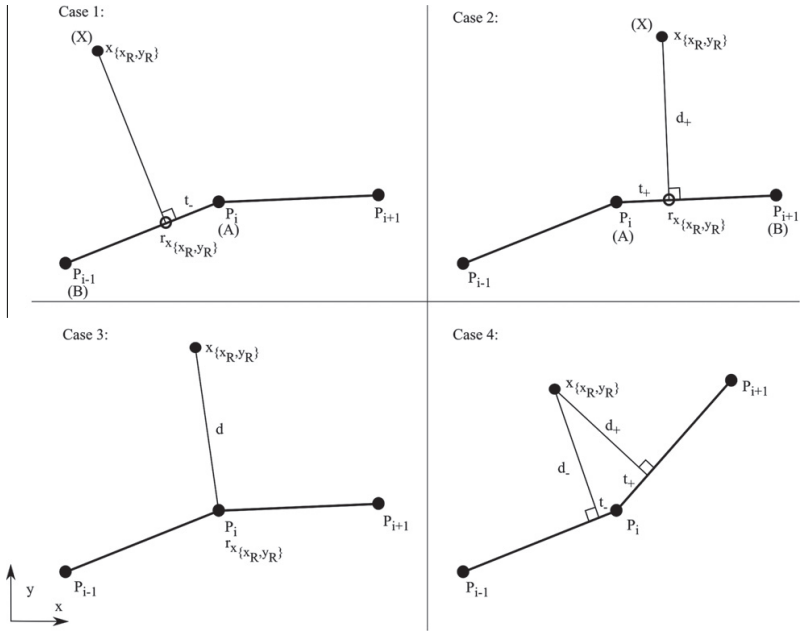

Fig. 4. Four different cases to calculate the trajectory point corresponding to the current state; Case 1: Position X is closest to the line $P_{i-1} - P_i$, Case 2: Position X is closest to the line $P_i - P_{i+1}$, Case 3: Position X is closest to path position P_i and Case 4: Inner curve.

the polynomial time interior-point method. The Lagrangian function of the problem is approximated quadratically by a sparse Hessian matrix, which is updated numerically using the Broyden–Fletcher–Goldfarb–Shanno (BFGS) method. The Jacobian matrices of the system equations and the cost function are, however, analytically solved in this research.

The time constants in vehicle control are very different from the applications where HQP has been reported to be used so far. Some modifications had to be made in order to fulfil strict time limits. The original software interface of the HQP was removed and a new one, which serves the purposes of this study better, was implemented. Also, because there is no guarantee of the computational time of the NMPC optimization, an interrupt routine was added. The timer is responsible for keeping the cycle time constant. If the time slot of the timer runs out and the NMPC has not yet acquired a new solution ($u = u^*(t_{k+1}|t_k)$), the optimization is interrupted and the previously calculated control values are used ($u = u^*(t_{k+1}|t_{k-1})$, notice that the index k is now increased and the control value used is different from that in the previous step). In the case of the interrupt, the length of the prediction horizon (M) is also decreased. After 10 feasible solutions, the prediction horizon starts to increase one step at the time. Vougioukas (2007) reported that the prediction horizon has to be more than 25 steps in order to be better than traditional control algorithms. In this case, the prediction horizon was set to be 30 steps at maximum and 10 steps minimum.

4. State estimation

The state of the controlled system cannot be directly measured. The obtained measurements are delayed at some specific amount of time. Also, the control outputs are delayed and the actuators include dynamics. The NMPC controller needs an accurate estimate of the state when the current control outputs affect the controlled system. Otherwise, the stability of the controller is uncertain.

4.1. Extended Kalman Filter

The Extended Kalman Filter (EKF) was used for the state estimation. The implemented EKF in this research follows the standard estimation methods. The general form of the estimated system model is:

$$\begin{aligned}\hat{x}(t_{k+1}) &= f_{est}(\hat{x}(t_k), u(t_k)) + w(t_k)\\ \hat{y}(t_k) &= h(\hat{x}(t_k)) + v(t_k),\end{aligned} \tag{24}$$

where f_{est} is the estimation model for the system and h is the measurement function. The difference from the prediction model used in the NMPC is that the estimation model includes noise terms ($w(t_k)$ and $v(t_k)$) both in the state equation and in the measurement equation. The noise terms are supposed to be independent and white Gaussian noise:

$$\begin{aligned}p(w(t_k)) &\sim N(0, Q(t_k))\\ p(v(t_k)) &\sim N(0, R(t_k)),\end{aligned} \tag{25}$$

where $Q(t_k)$ and $R(t_k)$ are the covariance matrices of the noises at time t_k.

Another difference is that the estimated state vector includes augmented delayed states in order to get the delayed measurements:

$$\hat{x}(t_k) = [x(t_k) \quad x(t_{k-1}) \quad x(t_{k-2}) \quad \cdots \quad x(t_{k-n})]^T, \tag{26}$$

where n is the number of delayed states and x is the state-vector of the system (Eq. (10)).

The estimation model predicts the new state of the system ($x(t_{k+1})$) with the model of the system (f in Eq. (12)) and moves the old states further within the augmented state vector:

$$f_{est}(\hat{x}(t_k), u(t_k)) = [f(x(t_k), u(t_k)) \quad x(t_k) \quad x(t_{k-1}) \quad \cdots \quad x(t_{k-n+1})]^T. \tag{27}$$

The measurement model picks up certain elements from the augmented state vector such that the delay of the corresponding measurement equals the true delay measured from the system:

$$h(\hat{x}(t_k)) = \begin{bmatrix} x_R(t_{k-\tau(x_R)}) \\ y_R(t_{k-\tau(y_R)}) \\ \theta(t_{k-\tau(\theta)}) \\ v_t(t_{k-\tau(v_t)}) \\ \alpha_t(t_{k-\tau(\alpha_t)}) \\ \beta(t_{k-\tau(\beta)}) \\ \gamma_t(t_{k-\tau(\gamma_t)}) \\ x_E(t_{k-\tau(x_E)}) \\ y_E(t_{k-\tau(y_E)}) \end{bmatrix}, \tag{28}$$

where $\tau(\cdot)$ is the delay (sampling periods) of the corresponding measurement.

4.2. Local measurement using laser scanner

A challenge in the estimation is to merge the global position measurement produced by the GPS and local measurement produced by the laser scanner. In order to do that, the route of the seed drill is recorded into the memory of the navigation system. The estimated position of the marking plough (x_P, y_P) and produced furrow can be calculated geometrically from the estimated (x_E, y_E) position and orientation of the seed drill (Eq. (9)). The estimated distance from the furrow can be calculated from the recorded furrow positions and estimated laser scanner position (x_L, y_L) in the same manner as the trajectory points were calculated from the path in the NMPC. However, in this case the direction of the distance-vector is known.

The laser scanner measures the vertical profile of the ground. The ground level is estimated from this profile by fitting a first degree polynomial to the profile by minimizing the MSE error. The lateral distance to the adjacent swath is found by fitting the prototype of the furrow profile to the residuals of the first degree polynomial fit (Backman et al., 2009).

The difference between the measured and estimated distances tells how much current and past estimations differ laterally at the angle perpendicular to the seed drill's current heading (Fig. 5). Correcting both estimates would require recalculating all the recorded estimates again in every estimation step. Because this would require too much computation time to do that in real time, only the current estimate is corrected through the EKF. The correction equations are:

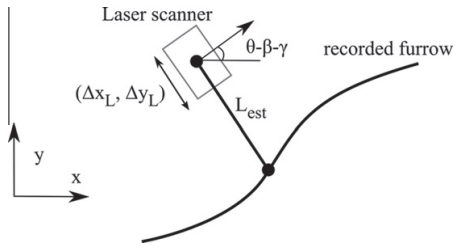

Fig. 5. Correcting the estimated position of the laser scanner using the laser scanner measurement and recorded furrow position. Notice, that L_{est} is not necessarily perpendicular to the furrow (as it is in the trajectory generation).

$$\Delta x_L = (L_{meas} - L_{est})\cos(\theta - \beta - \gamma_t)$$
$$\Delta y_L = (L_{meas} - L_{est})\sin(\theta - \beta - \gamma_t), \quad (29)$$

where L_{est} is the estimated lateral distance calculated based on recorded furrow positions and L_{meas} is the measured lateral distance. The correction values are used directly in the EKF as innovation terms, hence:

$$x_{E,meas}(t_k) = h(\hat{x}(t_k))_{\{x_E\}} + \Delta x_L$$
$$y_{E,meas}(t_k) = h(\hat{x}(t_k))_{\{y_E\}} + \Delta y_L, \quad (30)$$

where $x_{E,meas}$ is the x coordinate and $y_{E,meas}$ is the y coordinate of a pseudo measurement of the laser scanner.

4.3. Heading estimation

In the early experiments it was found that the accuracy of heading measurement is crucial for the accuracy of path tracking. From GPS a heading of vehicle can be acquired, but depending on the GPS receiver this measurement may be poor, especially when driving at slow speeds. Furthermore, when the vehicle is not moving, no heading can be measured by using only a single GPS.

In an earlier project, an improved positioning estimation system prototype was developed (Oksanen et al., 2005). In the project, a low cost GPS receiver was integrated with an inertial measurement unit (IMU), tractor measurements and a kinematic model. The position and attitude of a vehicle was estimated using an Extended Kalman Filter. It was reported that the main problem in the estimation was related to the non-Gaussian, non-white property of GPS positioning noise. However, the system was able to improve the heading remarkably compared to raw GPS heading, as the IMU contained a 3D magnetic field sensor that could be also used to estimate the absolute heading. Additionally, the 3D gyroscope gave information about the rate of heading change.

In the experiments reported below, the same system with some modifications was used to estimate the heading of the tractor. The heading estimate utilizes positioning, velocity and heading information from the RTK-GPS in the tractor, angular rate and magnetic field and attitude information from the IMU as well as velocity information from the tractor. The system for positioning estimation first transforms all the measurements to the tractor coordinate system, and uses an Extended Kalman Filter to estimate the position and heading. However, only the heading information from this EKF filter is used in NMPC related state estimation; the positioning measurement from the RTK-GPS is directly used.

For heading estimation, two solutions are needed: a variable covariance in the measurement covariance matrix related to the GPS heading measurement, and a 180 deg bias on the GPS heading measurement when the tractor is moving backwards. If the estimated velocity is slow, the covariance is set high, as the faster the receiver moves the better the heading measurement. In the following experiments, a threshold of 1 m/s was used. The only source of true direction of travel comes from the tractor wheel speed sensor; over an ISO 11783 network. The other velocity measurements are the tractor ground speed sensor and the GPS velocity measurement, but none of those contain any information about the true direction of travel.

5. Comparative control algorithms

For comparison, alternative control algorithms were implemented for both the tractor and the implement. These control algorithms are independent from each other. However, in the test, these control algorithms were used together. The combination of these control algorithms is referred later on as the Target Point (TP) algorithm. The tractor control algorithm is similar to the Pure-Pursuit method (Coulter, 1992). The implemented algorithm tries to calculate the steering angle so, that some desired "target point" is reached (Fig. 6). The steering angle is calculated:

$$a = \frac{2x}{l^2}, \quad (31)$$

where x is the lateral distance to the path at the distance l ahead of the tractor (Fig. 6). The look-ahead distance l is calculated:

$$l = \min(v * f_{dist}, l_{min}), \quad (32)$$

where v is the current driving speed, f_{dist} is the distance factor and l_{min} minimum allowed distance. In the tests, f_{dist} was set to 2 and l_{min} was set to 2.

As with the tractor control algorithm, the implement control algorithm is nonlinearly dependent on the error variable and has a geometric meaning (Fig. 7). The control angle of the drawbar is calculated as:

$$\gamma_{new} = \sin^{-1}\left(\sin(\gamma_{old}) - \frac{L_{est}}{c}\right), \quad (33)$$

where γ_{old} is the current control angle, L_{est} is the estimated distance to the swath edge and c is the length of the drawbar (Fig. 7).

6. Results

The methods were evaluated in two different ways: a comparison between the traditional path tracking method and the method proposed in this article (Section 6.1), and, the effect of the laser scanner measurements on the state estimate (Section 6.2).

The controllers were preliminary tested and tuned in a simulation environment. The final tunings were performed with real world environment and with the actual hardware.

The dimensions of the test vehicle (Fig. 2) are following:

a = 2.8 [m]	l_x = 2.7 [m]
b = 1.7 [m]	l_y = 1.48 [m]
c = 2.3 [m]	p_x = 1.1 [m]
d = 3.3 [m]	p_y = 1.48 [m]

The physical limitations of the control variables and joint angles are:

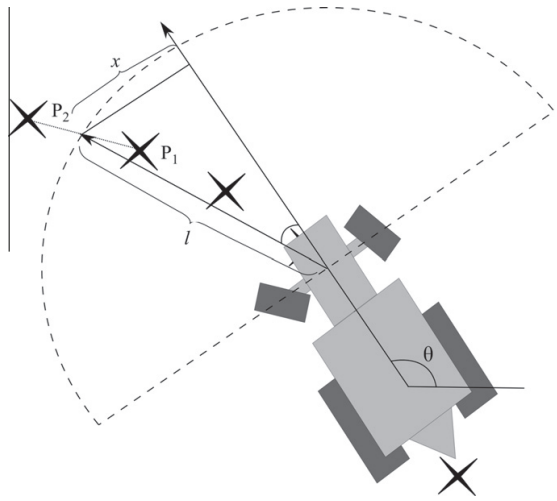

Fig. 6. The geometric presentation of the Target Point algorithm.

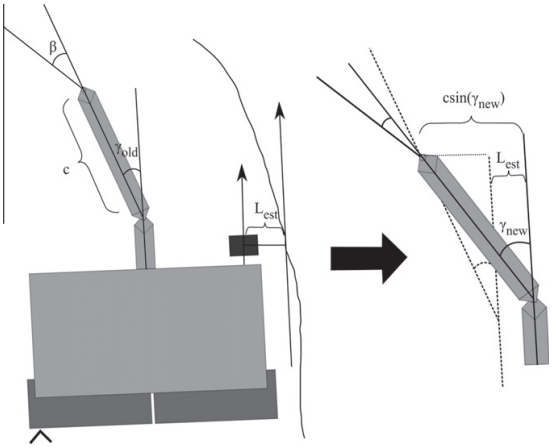

Fig. 7. The geometric presentation of the drawbar control algorithm.

$\max|\dot{v}| = 1$ [m/s^2] $\max|v| = 5$ [m/s] $\max|\beta| = 1.57$ [rad]
$\max|\dot{\alpha}| = 0.7$ [rad/s] $\max|\alpha| = 0.7$ [rad] $\max|\gamma| = 0.33$ [rad]
$\max|\dot{\gamma}| = 0.33$ [rad/s]

The standard deviations of the state variables and measurements were empirically fitted by filtering recorded measurements and manually fine-tuned to get satisfactory estimation results. The following standard deviations were obtained in the test drives:

$x_R = 0.002$ [m]
$y_R = 0.002$ [m]
$\theta = 0.00002$ [rad]
$v = 0.00007$ [m/s]
$\alpha = 0.009$ [rad]
$\delta = 0.00001$
$\beta = 0.000001$ [rad]
$\gamma = 0.000002$ [rad]
$x_E = 1 * 10^{-10}$ [m]
$y_E = 1 * 10^{-10}$ [m]

$x_{R,meas} = 0.03$ [m]
$y_{R,meas} = 0.03$ [m]
$\theta_{meas} = 0.0035$ [rad]
$v_{meas} = 0.000067$ [m/s]
$\alpha_{meas} = 0.0066$ [rad]
$\beta_{meas} = 0.0055$ [rad]
$\gamma_{meas} = 0.0002$ [rad]
$x_{E,meas} = 0.038$ [m]
$y_{E,meas} = 0.038$ [m]

The measurement delays were identified concurrently with standard deviation measurements and the following delays were found:

$\tau(x_{R,meas}) = 300$ [ms] $\tau(v_{meas}) = 100$ [ms] $\tau(\gamma_{meas}) = 200$ [ms]
$\tau(y_{R,meas}) = 300$ [ms] $\tau(\alpha_{meas}) = 100$ [ms] $\tau(x_{E,meas}) = 0$ [ms]
$\tau(\theta_{meas}) = 500$ [ms] $\tau(\beta_{meas}) = 200$ [ms] $\tau(y_{E,meas}) = 0$ [ms]

The weights of the NMPC controller were experimentally searched. The following weights were used in test drives:

$R_{\{\dot{v}\}} = 0.02$ $R_{\{v\}} = 20$ $Q_{\{x_R,y_R\}} = 0.1$
$R_{\{\dot{\alpha}\}} = 0.004$ $R_{\{\alpha\}} = 0.04$ $Q_{\{x_E,y_E\}} = 0.005$
$R_{\{\dot{\gamma}\}} = 0.004$ $R_{\{\gamma\}} = 0.001$ $Q_{\{\theta\}} = 0.1$

where $Q_{\{x_R,y_R\}}$ denotes the weighting factor of the lateral error of the tractor and $Q_{\{x_E,y_E\}}$ denotes the weighting factor lateral error of the implement. The variable $Q_{\{\theta\}}$ denotes the weighting of heading error of the tractor. $R_{\{v\}}$, $R_{\{\alpha\}}$ and $R_{\{\gamma\}}$ are weights for the steady state control values. $R_{\{\dot{v}\}}$, $R_{\{\dot{\alpha}\}}$ and $R_{\{\dot{\gamma}\}}$ are weights for the optimized control values changes.

6.1. Comparison of different path tracking methods

The different path tracking methods were compared in two test procedures. In the first test, denoted in this study as "straight path", the driver made the first straight driving line, a turn in a headland and switched the guidance system on. After that, the speed was kept constant and the previous driving line was followed for 30 m. In the second test, denoted in this study as "curved path", the driver started the test in the same way as in the first, by making the first driving line. At this time, the driving line was curved with a 50 m wavelength and a 4 m amplitude (Fig. 8). The guidance system followed the driving line for the next four driving lines, and also when executing the headland turnings.

The results of the first tests are presented in Figs. 9–11. The figures represent the tracking errors of the tractor (Fig. 9) and the trailer (Fig. 10) calculated from the state estimates, i.e. control error, and the distance to the adjacent driving line (Fig. 11) calculated from the raw GPS measurements, i.e. absolute error. The measurements are visualized in the form of a box-and-whiskers plot. The box in the plot represents the middlemost half of the data and the line inside the box represents the median value. The whiskers represent the smallest value and the largest value. The crosses represent outliers. The tracking errors were calculated in real time from the state estimation of the tractor–trailer system and the same measurements were used as error values in controllers. The distance to the adjacent driving line is calculated afterwards from the raw VRS-GPS measurements. The target distance or the working width was 2.95 m. All measurements are taken at 100 ms intervals.

The results of the second tests are given in Figs. 12–14. The figures represent the same measurements as in the first tests; the tracking error of the tractor (Fig. 12) and the trailer (Fig. 13) and the distance to the adjacent driving line (Fig. 14.). All of the measurements were taken under the steady-state conditions after the transition from the headland path.

6.2. Estimate correction with laser measurements

The position estimation with and without laser scanner measurements was analyzed with similar test drives as the path tracking comparison. The driving speed was 8 km/h in every test. For clarity, unreliable laser scanner measurements are removed from the pictures and from mean error calculations as well. The quality

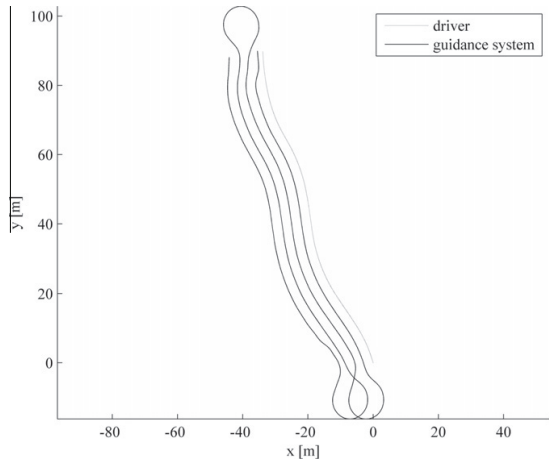

Fig. 8. Curved driving line.

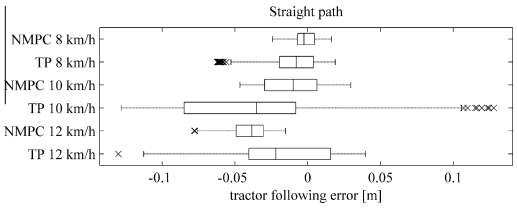

Fig. 9. Box-and-whiskers plot of the tracking errors of the tractor in straight-path-following tests.

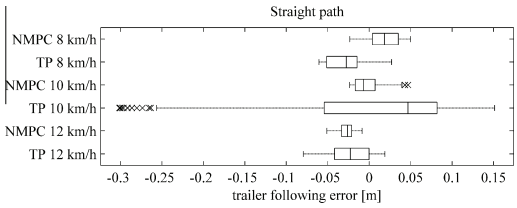

Fig. 10. Box-and-whiskers plot of the tracking error of the trailer in straight-path-following tests.

value 0.4 was considered to be the best threshold value to distinguish between unreliable and reliable measurements.

Table 1 presents the same results as in Fig. 15 (the straight line following test) and Fig. 16 (the curved line following test). Additionally presented in the table are the mean and the variance of the calculated tracking errors of the tractor and the trailer. In the table, the column labelled as 'Laser' consists of tracking errors calculated directly from the laser scanner measurements. The column labelled as 'Laser Diff.' is the calculated difference between the estimated tracking error of the trailer and the laser scanner measurements. The column labelled as 'VRS Diff.' Is the calculated difference between the estimated tractor positions and the true delayed measurements. The statistical values for the laser scanner measurement and the difference between laser and estimated trailer error are calculated only from the values when laser scanner measurement is considered to be acceptable whereas other values are calculated from the whole time slot.

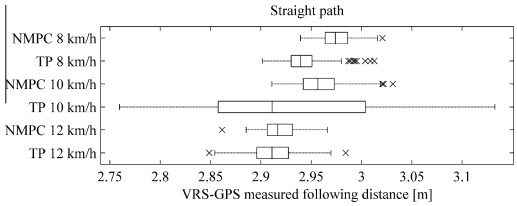

Fig. 11. Box-and-whiskers plot of the distance to the adjacent driving line measured by VRS-GPS in straight-path-following tests.

7. Discussion

The goal was to develop a navigation system for a tractor –trailer system, which is able to drive at least 12 km/h with less than 10 cm lateral error. The results show, that the goal is reached most of the time. However, there are situations where the controller was not able to keep the lateral error within the accepted range. This is caused mainly from the slow dynamics of the drawbar and uncertainties in the measurements. Results show also the superiority of the proposed method compared to the simple geometrical path tracking and separate implement control methods. However, the cost of the better accuracy is the complexity of the system. The algorithm presented in this study is computationally a lot heavier and not equally reliable as the comparing methods. It is recommendable to implement a backup method, which is simpler and more robust but not necessarily useful for accurate path tracking. The backup system could take over the control, when the NMPC fails in real-time.

The method for the estimating the state seemed to be sufficient for the required path tracking accuracy. As shown in the results, the controller was able to keep the errors at the same ranges in both cases: the laser correction on and off. But in the straight line following tests, the standard deviation was much smaller than in the curved line following tests. The most interesting values are the mean values and standard deviations of the difference between the estimated trailer errors and laser scanner measurements (Table 1, column "Laser Diff."). The deviation is more significant when the laser scanner correction is off. This implicates that the estimated position of the trailer is not correct when the laser scanner is not used if it is assumed that laser scanner measurement is correct. By using the laser scanner, more reliable position estimation is achieved. The laser measurement system would be more usefully and justified, if the GPS-device would be less accurate or other measurements would include more noise or systematic errors. Fur-

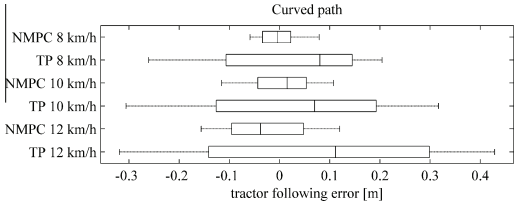

Fig. 12. Box-and-whiskers plot of the tracking error of the tractor in curved-path-following tests.

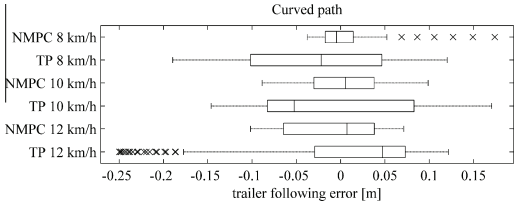

Fig. 13. Box-and-whiskers plot of the tracking error of the trailer in curved-path-following tests.

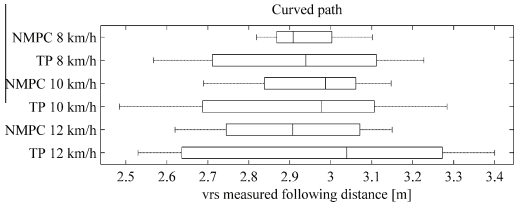

Fig. 14. Box-and-whiskers plot of the distance to the adjacent driving line measured by VRS-GPS in curved-path-following tests.

Table 1
Test results in statistical form.

	Laser correction	Laser OK [%]	Tractor $\mu(\sigma)$ [$m(m)$]	Trailer $\mu(\sigma)$ [$m(m)$]	Laser $\mu(\sigma)$ [$m(m)$]	Laser Diff. $\mu(\sigma)$ [$m(m)$]	VRS Diff. $\mu(\sigma)$ [$m(m)$]
Straight line	ON	77.5	0.022 (0.020)	−0.004 (0.014)	−0.010 (0.017)	0.005 (0.010)	0.001 (0.013)
	OFF	85	0.051 (0.028)	0.028 (0.013)	−0.013 (0.012)	0.041 (0.020)	0.006 (0.011)
Curved line	ON	52.8	0.002 (0.063)	−0.037 (0.108)	−0.056 (0.108)	−0.005 (0.024)	0.003 (0.022)
	OFF	49.2	0.031 (0.073)	0.021 (0.076)	−0.007 (0.102)	0.004 (0.054)	0.011 (0.022)

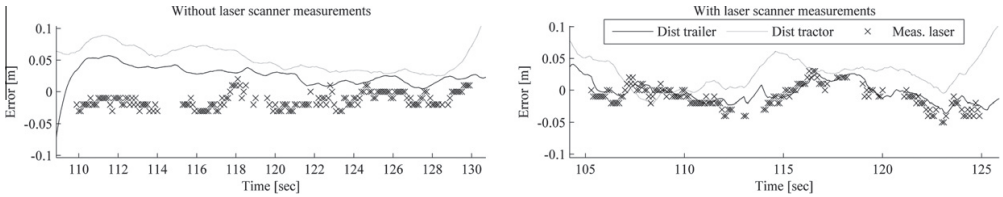

Fig. 15. Tracking errors in straight line following tests without (on the left) and with (on the right) laser scanner measurements in the Kalman-filter. Errors are measured by laser scanner and VRS-GPS.

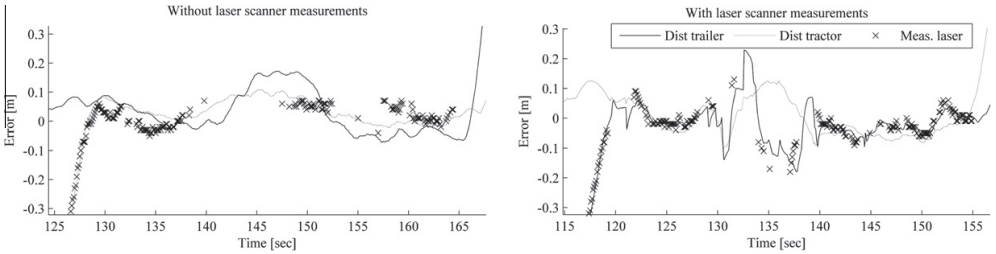

Fig. 16. Tracking errors in curved line following tests without (on the left) and with (on the right) laser scanner measurements in the Kalman-filter. The tractor went over the mark-furrow and the laser scanner was unable to measure the distance for the whole time.

ther investigation is needed to determine how stable the estimator would be if a cheaper and less accurate GPS-device is used.

Because of the delays, the estimation method predicts the future state of the system. The standard deviation of the difference between the estimated positions and VRS-GPS measurements (Table 1, column "VRS Diff.") are the same order of magnitude as the VRS-GPS accuracy by itself, so it cannot be said for sure which one is more accurate without other additional measurements. But it can be said that the prediction ahead does not increase the error or reduce the accuracy.

In the NMPC, the deviation of the tractor from the path was also in the cost function, although it is not the objective of the control problem. This is because the system would not be stable otherwise. Also the weight ratio between tractor and trailer was empirically searched to get sufficient tracking accuracy of the trailer on the one hand and stable behaviour of the tractor on the other. An alternative final state constraint or infinite prediction horizon would also work, but those are impractical to implement.

The implementation of the cost function of the NMPC controller is similar to the commonly used potential field method (Murphy, 2000). The difference is that the NMPC controller predicts the future states and the cost function is calculated in several positions ahead of the tractor's current position. By this way, the tractor is able to follow the path accurately along an almost optimal trajectory with respect to the physical constraints. Moreover, the avoidance of static obstacles is easy to implement using the scheme of this study (Vougioukas, 2007). Application for the avoidance of other moving working machines is also possible, but may require more work as compared to avoiding static obstacles (Vougioukas, 2009).

8. Conclusions

In this article a path tracking method was proposed for a tractor–trailer system by using a Nonlinear Model Predictive Controller. The research is different to other researches where NMPC was used in that the objective is to keep both, the tractor and the trailer, on a path. This study is useful because unlike other similar research where a tractor–trailer system is controlled, the uncertainties in the environment, due to slipping and sliding, is considered and additionally, the control problem is consider as a multivariate nonlinear control problem rather than as a separate or a linearized problem.

The proposed method to calculate the cost function and the trajectory in the NMPC makes the controller suitable for path tracking, where the desired positions and the time are not coupled. Other similar researches with NMPC typically use the controller for trajectory tracking, where the desired positions and the time are coupled. A novel variable horizon length was also used in this research. This proposed method makes it possible to use an optimal length prediction horizon with respect to the computational capacity. The horizon is decreased when the capacity runs out and increased when the solution is achieved in a shorter time instance.

The NMPC requires an accurate state estimate in order to be stable. The global positioning system, GPS, was used together with the model of the system in an Extended Kalman Filter. The heading

estimation of GPS was improved by using an inertial measurement unit and separate EKF filter. The position estimate of the trailer was also improved by using a local relative measurement by recognizing the adjacent driving lines using a 2D laser scanner.

The results showed that the NMPC is a feasible method to realize path tracking. The lateral error of the trailer was well below the required 10 cm in straight paths and within the boundaries in curved paths up to 12 km/h driving speed. The objectives were therefore, achieved with the presented system.

Acknowledgements

A part of this research is done in the project Agromassi that is part of FIMECC-program EFFIMA. A part of this research is also funded by the Graduate School in Electronics, Telecommunications and Automation (GETA). GETA is a post graduate programme offered jointly by five universities: Aalto University School of Electrical Engineering, Tampere University of Technology and the Universities of Oulu, Turku and Jyväskylä.

References

Backman, J., Oksanen, T., Visala, A., 2009. Parallel guidance system for tractor–trailer system with active joint. In: van Henten, E.J., Goense, D., Lokhorst, C. (Eds.), Precision Agriculture '09. Proceedings of the Joint International Agricultural Conference. Wageningen Academic Publishers, Wageningen, Netherlands, pp. 615–622.

Bell, T., 1999. Precision robotic control of agricultural vehicles on realistic farm trajectory. Ph.D. Dissertation, Stanford University, USA.

Bevly, D.M., 2001. High speed, dead reckoning, and towed implement control for automatically steered farm tractors using GPS. Ph.D. Dissertation, Stanford University, USA.

Cariou, C., Lenain, R., Thuilot, B., Martinet, P., 2010. Autonomous maneuver of a farm vehicle with a trailed implement: motion planner and lateral–longitudinal controllers. In: IEEE International Conference on Robotics and Automation, Anchorage, Alaska, USA, pp. 3819–3824.

Coulter, R.C., 1992. Implementation of the Pure Pursuit Path Tracking Algorithm. Technical Report CMU-RI-TR-92-01, Robotics Institute, Carnegie Mellon University, USA.

Deere & Company, 2009a. iGuide Operators Manual. <http://manuals.deere.com/omview/OMPFP10808_19/> (accessed 16.09.11).

Deere & Company, 2009b. iSteer Operators Manual. <http://manuals.deere.com/omview/OMZ200263_19/> (accessed 16.09.11).

Falcone, P., Borrelli, F., Asgari, J., Tseng, H.E., Hrovat, D., 2007. Predictive active steering control for autonomous vehicle system. IEEE Transaction on Control System Technology 15 (3), 566–580.

Franke, R., Arnold, E., 1997. Applying new numerical algorithms to the solution of discrete-time optimal control problems. In: Warwick, K., Kárný, M. (Eds.), Computer-Intensive Methods in Control and Signal Processing: The Curse of Dimensionality. Birkhäuser Verlag, Basel, pp. 105–118.

Franke, R., Arnold, E., 2008. HQP: a solver for sparse nonlinear optimization. <http://hqp.sourceforge.net/> (accessed 15.02.11).

Gu, D., Hu, H., 2006. Receding horizon tracking control of wheeled mobile robots. IEEE Transaction on Control System Technology 13 (4), 743–749.

Karkee, M., Steward, B.L., 2010. Study of the open and closed loop characteristics of a tractor and a single axle towed implement system. Journal of Terramechanics 47 (6), 379–393.

Keviczky, T., Falcone, P., Borrelli, F., Asgari, J., Hrovat, D., 2006. Predictive control approach to autonomous vehicle steering. In: Proceedings the 2006 American Control Conference ACC. Minneapolis, Minnesota, USA, pp. 4670–4675.

Kim, B., Necsulescu, D., Sasiadek., J., 2001. Model predictive control of an autonomous vehicle. In: Proceedings of 2001 IEEE/ASME International Conference on Advanced Intelligent Mechatronics, Como, Italy, pp. 1279–1284.

Klančar, G., Škrjanc, I., 2007. Tracking-error model-based predictive control for mobile robots in real time. Robotics and Autonomous Systems 55 (6), 460–469.

Kühne, F., Gomes da Silva Jr., J.M., Lages, W.F., 2005a. Mobile Robot Trajectory Tracking Using Model Predictive Control. VII SBAI II LARS, São Luís, Brazil.

Kühne, F., Lages, W.F., Gomes da Silva Jr., J.M., 2005b. Point stabilization of mobile robots with nonlinear model predictive control. In: Proceedings of 2005 IEEE International Conference on Mechatronics and Automation, vol. 3, Niagara Falls, Canada, pp. 1163–1168.

Lenain, R., Thuilot, B., Cariou, C., Martinet, P., 2005. Model predictive control for vehicle guidance in presence of sliding: application to farm vehicles path tracking. In: Proceedings of the 2005 IEEE International Conference on Robotics and Automation. ICRA, Barcelona, Spain, pp. 885–890.

Murphy, R.R., 2000. Introduction to AI Robotics. MIT Press, Cambridge, MA, USA.

Nagy, Z.K., Mahn, B., Franke, R., Allgöwer, F., 2007. Evaluation study of an efficient output feedback nonlinear model predictive control for temperature tracking in an industrial batch reactor. Control Engineering Practice 15 (7), 839–850.

Oksanen, T., Linja, M., Visala, A., 2005. Low-cost positioning system for agricultural vehicles. In: Proceedings of The IEEE International Symposium on Computational Intelligence in Robotics and Automation. CIRA, Espoo, Finland, pp. 297–302.

Siew, K.W., Katupitiya, J., Eaton, R., Pota, H., 2009. Simulation of an articulated tractor-implement-trailer model under the influence of lateral disturbances. In: IEEE/ASME International Conference on Advanced Intelligent Mechatronics, Singapore, pp. 951–956.

Schittkowski, K., 1983. On the convergence of a sequential quadratic programming method with an augmented Lagrangian line search function. A Journal of Mathematical Programming and Operations Research 14 (2), 197–216.

Snider, J.M., 2009. Automatic Steering Methods for Autonomous Automobile Path Tracking. Technical Report CMU-RI-TR-09-08, Robotics Institute, Carnegie Mellon University, Pittsburgh, PA, USA.

Vougioukas, S.G., 2007. Reactive trajectory tracking for mobile robots based on non linear model predictive control. In: 2007 IEEE International Conference on Robotics and Automation. ICRA, Roma, Italy, p. 3074.

Vougioukas, S.G., 2009. A framework for motion coordination of small teams of agricultural robots. In: van Henten, E.J., Goense, D., Lokhorst, C. (Eds.), Precision Agriculture '09. Proceedings of the Joint International Agricultural Conference. Wageningen Academic Publishers, Wageningen, Netherlands, pp. 585–593.

Wong, J.Y., 2008. Theory of Ground Vehicles, fourth ed. John Wiley and Sons.